Microstructural Characterization and Mechanical Performance of Cemented Carbide Steel Joints in Mining Tools Using TIG and MIG Welding Techniques

Frendy Edo Herlanto and Agus Dwi Anggono*

Department of Mechanical Engineering, Universitas Muhammadiyah Surakarta, Indonesia
Email: u100220011@student.ums.ac.id (F.E.H.); ada126@ums.ac.id (A.D.A.)
*Corresponding author

***Abstract*—Cemented Carbide (WC-Co) is widely used in the mining and metal-forming industries due to its exceptional hardness, wear resistance, and toughness. Cemented carbide is often combined with carbon steel to create tools such as drill bits and lathe chisels to optimize production costs. However, the joining process between these materials presents significant challenges, primarily related to brittleness and cracking. This study explores the use of Tungsten Inert Gas (TIG) and Metal Inert Gas (MIG) welding to join cemented carbide with carbon steel. Microstructural analysis using Scanning Electron Microscope (SEM) and Energy Dispersive Spectroscopy (EDS) revealed the formation of a new layer at the interface, enriched with C, O, Fe, and W elements. Mechanical testing, including shear strength and microhardness assessments, demonstrated that both welding methods increased the hardness of the steel and cemented carbide at the filler metal interface. The difference in hardness values between the filler metal for TIG and MIG welding was 37.14%, with TIG welding yielding the highest hardness. In terms of shear strength, MIG welding exhibited superior performance, achieving a maximum value of 387.4 MPa. Fracture patterns observed in both welding methods predominantly occurred within the cemented carbide/WC-Co material. These findings provide insights into the mechanical behavior and microstructural characteristics of welded joints between cemented carbide and steel, contributing to the development of more reliable and durable industrial tools.**

***Keywords*—Cemented Carbide (WC-Co), Tungsten Inert Gas (TIG), Metal Inert Gas (MIG) welding, microstructural, Shear strength, hardness, steel-carbide joint**

I. Introduction

In recent years, a material called cemented carbide WC-Co has become popular in the development of cutting tools and drill bits. The properties of cemented carbide include high hardness, better wear resistance, and high durability. The industrial manufacturing process is often carried out with high-speed material cutters and metal-forming tools. Cemented carbide is also commonly used as the primary material (die, ring, roll, blade, slitter, rotor, stator) used in the mining and oil drilling industries [1]. Finally, cemented carbide is also trusted for its high strength and durability in many hydraulic applications of jet engine components and automotive components (fuel pumps, fuel injectors, compressors, and valve assemblies).

Cemented Carbide (WC-Co) is often combined with structural steel. By combining cemented carbide with structural steel, high-quality products can be produced, and production costs can be reduced [2, 3]. Joining cemented carbide with steel presents a number of technical challenges because they have different physical properties and characteristics, requiring high-quality joining techniques to avoid brittleness and cracking [4, 5].

II. Literature Review

In relation to the connection of cemented carbide with steel, which has different properties and characteristics, researchers have carried out many approaches in the connection process using the brazing welding method [6, 7]. Friction Stir Welding [8], Diffusion Bonding [9], and Sinter Bonding. The use of the welding process in the connection can produce high temperatures, causing changes in the microstructure of the cemented carbide part [10, 11]. The results of Scanning Electron Microscope (SEM) observations on the YG30 connection with 1045 steel using the TIG connection method formed WC particles in the Heat-Affected Zone (HAZ) section, which were affected by W, C, and Fe, Co, Ni due to the heat generated by the welding process. The research was conducted [12]. The connection of WC-Co with steel using a brazing temperature of 740 °C for 30 s causes a change in the chemical composition of the filler metal alloy [13]. WC migration occurs not only in the fusion zone but also in the HAZ, especially near the top surface, which causes gradient layers, η phases, and tungsten precipitation-dissolution on the WC surface. The results

Manuscript received September 18, 2024; revised November 11, 2024; accepted December 17, 2024; published March 20, 2025.

also show that the fusion zone can heal cracks during robotic MIG welding [14].

Ni-coated Single Bond Zn alloy was used as an interlayer to bond cemented carbide and steel. The results show that the added Ni promotes the formation of diffusion zones, which has a positive effect on brazing [15]. Two-layer Ti/Ni/Ti alloy for partial liquid phase bonding of cemented carbide and 40Cr steel. The results showed that the active phase of the Ti layer increased the ability and rate of metallurgical reactions with both base materials [16]. Ag filler metal is used for WC-Co/C steel joints by high-frequency induction brazing. The strengthening mechanism involves diffusion strengthening through island-like α-Cu solid solution distributed in the fusion region and the strengthening effect of the α-Cu layer at the interface [17]. The impact of interlayer (pure Ni) on the shear strength of WC-Co/40Cr joints was found to decrease sharply with increasing interlayer thickness [8].

Based on literature studies, there have been many discussions about the welding method of Cemented Carbide WC-Co and steel produced by modifying the joint structure. Tungsten Inert Gas (TIG) and Metal Inert Gas (MIG) welding have reasonable current control, which will produce stable heat input for the materials being joined. This technique allows the technique to produce homogeneous microstructure joints, especially for welding different materials. Therefore, a comparative study of the mechanical properties of ER70S-6 filler metal specimens was conducted. Observation of the microstructure and testing of mechanical properties focused on the properties of the joints in the hardness test and the shear strength test of the welding results. Test specimens produced using two types of welding processes, namely TIG and MIG, were used to conduct a comparative study.

III. Materials and Methods

This research was conducted through experimental procedures utilizing Metal Inert Gas (MIG) and Tungsten Inert Gas (TIG) welding methods. The base material for the specimens was cemented carbide in the form of YG6 tips, sourced from Zigong Cemented Carbide Corp (ZGCC), China, with dimensions of 25×15×8 mm. The selected cemented carbide material is consistent with that used in previous studies [18]. The filler metal employed was ER70S-6 electrode wire, which complies with AWS A5.18 standards. Its chemical composition includes iron, carbon, manganese, silicon, and other alloying elements that enhance mechanical properties and tensile strength.

Two welding methods were applied for the joining process. Utilizing continuously fed filler wire that also served as the electrode, the first method of welding was MIG. During this process, heat is generated between the filler wire and the parent metal, facilitating the weld. The second method, TIG welding, involved an electric arc welding process using a tungsten electrode to generate heat. An inert shielding gas, either argon (Ar), helium (He), or a combination of both, was used to protect the weld area from oxidation and contamination [19].

The specific welding parameters employed for the preparation of the research specimens are detailed in Table I. These parameters were optimized to ensure consistent welding quality across the different techniques used in this study.

TABLE I. Welding Parameters

Parameter	Specimen 1	Specimen 2
Welding process	MIG	TIG
Connection Type	Lap Joint	Lap Joint
Filler metal	ER70S-6	ER70S-6
Fillet Diameter	1.0 mm	2.0mm
Electric current	80 A	80 A
Shielding gas	CO_2	Argon Gas
Welding position	1G (Down Hand)	1G (Down Hand)

Material preparation is crucial for attaining optimal joint outcomes. An essential procedure involves one-way sanding of carbon steel and cemented carbide components using 200–400 grit sandpaper to eliminate contaminants, including dust, oil, and water. Furthermore, carbon steel and cemented carbide must be immersed in an acetone solution to cleanse the material's surface prior to the commencement of the welding process. The collaborative method employed in welding carbon steel and cemented carbide utilizes a laboratory joint type of connection, as illustrated in Fig. 1. The JIG tool stabilizes the material during the welding process. All materials must be accurately positioned to prevent errors in the welding process.

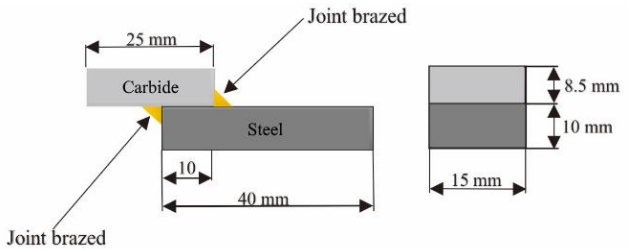

Fig. 1. Lap joins design for specimens.

Microstructure observation is employed to discover and examine the microstructure within the brazed joint region. This work utilized a Scanning Electron Microscope (SEM) with Energy Dispersive Spectroscopy (EDS) to ascertain the chemical composition in the joint area of the test specimen, achieving high image resolution. Moreover, Scanning Electron Microscopy (SEM) facilitates elemental analysis through the application of Energy-Dispersive Spectroscopy (EDS) technology. This method enables the authors to determine and measure the chemical constituents of the material, so yielding critical insights into its makeup. The SEM-EDS apparatus can accurately determine each element and phase configuration by examining the elemental distribution on the sample surface. This method is highly effective for material characterization and the examination of chemical processes, phase transitions, or contamination. Prior to the microstructural inspection, the specimen underwent preparatory processes, including grinding, sanding, polishing, and etching. The specimen's surface was initially abraded with a diamond grinding wheel. The

specimen's surface was abraded using sandpaper with a grit range of 200 to 2000. The sanded surface was refined with aliphatic hydrocarbons. The etching solution employed was a mixture of 98% alcohol and 2% nitric acid.

Shear compression testing is a test to determine the strength of the welding joint. In the shear compression test, the fracture results can be seen in each test specimen, each test object on the carbon steel welding joint, and cemented carbide on the TIG and MIG welding joints. The results of the shear test are generally the strength parameters of the welding joint results. Shear strength testing is carried out using a Universal Testing Machine (UTM). Illustration of shear strength testing as in Fig. 2. where the testing process on the material is pressed through one direction of force until there is a process of changing the shape and shifting of the object or changing the position of the starting point and the final position of the specimen object to determine the characteristics and mechanical properties of the welding results.

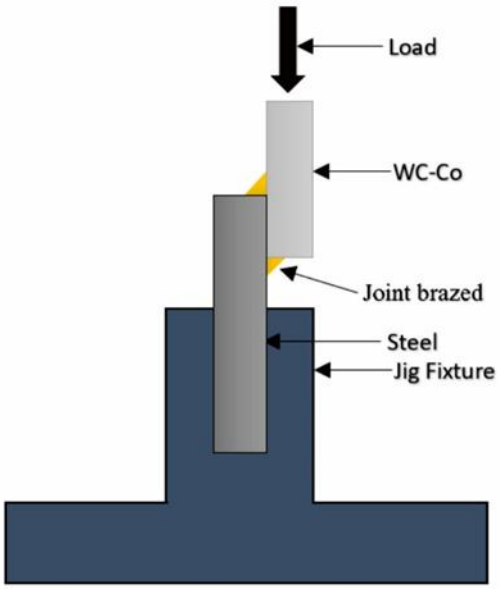

Fig. 2. Illustration of shear strength testing.

Vickers testing is conducted utilizing a hardness tester located at the Metal Testing Laboratory. This hardness test determines the material's hardness level, allowing for the assessment of its ductility or brittleness based on the hardness values obtained. A material's increased hardness value correlates with greater brittleness. Vickers testing is conducted to assess the welding outcomes of carbon steel and cemented carbide. The data acquired manifests as a distribution of hardness present in the weld material and the welded metal for each variant of TIG and MIG welding techniques. This hardness test is conducted using one test material for each variant of the welding type. Data is collected on each carbon steel material, filler metal, and cemented carbide at five pressure points, with a separation of five microns between each point. This hardness test occupies the top place. Testing is conducted with each specimen comprising a total of fifteen points. Hardness testing is performed utilizing the micro Vickers method with a load of 9.8 kgf and a duration of 15 s, in accordance with the ASTM E92 standard. The testing apparatus has been digitized, eliminating the necessity to refine the surface to measure the width and depth of holes resulting from crystal impacts with the test instrument.

IV. Result and Discussion

This study investigates the effects of two different welding methods—MIG and TIG—on the interface joint between carbon steel and carbide materials using the filler alloy ER70S-6.

A. Microstructure Analysis

Fig. 3 illustrates the microstructure of the interface joint between the ER70S-6 filler and the carbide material. SEM observations reveal that both MIG and TIG welding methods produce new layers with distinct characteristics. Specifically, TIG welding results in a homogeneous metallurgical bond without visible cracks or porosity, whereas MIG welding produces new layers with noticeable cracks.

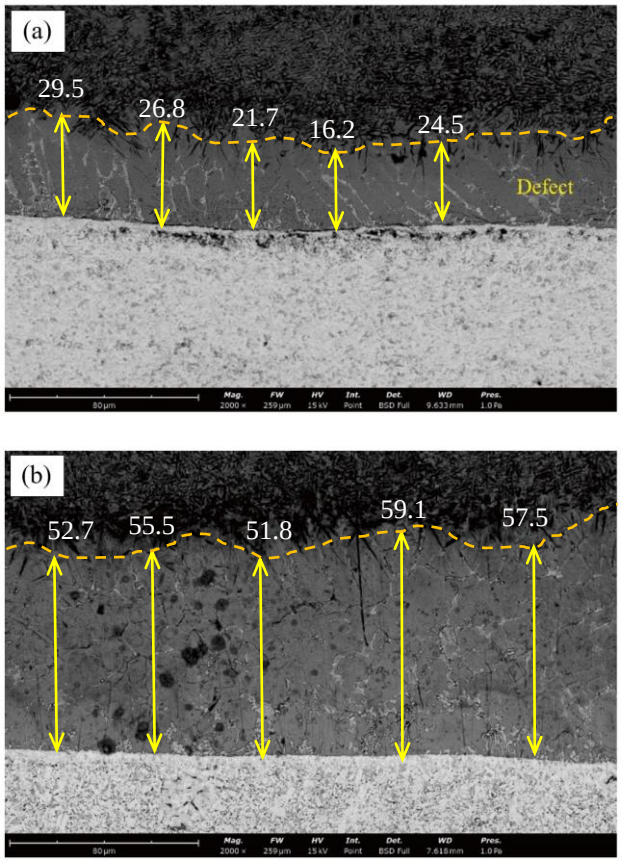

Fig. 3. Comparison of welding results at the carbide interface and filler material using two techniques: (a) MIG and (b) TIG welding.

The distinction is further highlighted by the average measurements obtained using ImageJ software, which indicate that MIG welding creates a new layer with a thickness of 23.7 µm. This value is derived from the average of five measurements: 29.5, 26.8, 21.7, 16.2, and 24.5 µm as shown in Fig. 3(a). The intermetallic layer

measurements were recorded as 52.7, 55.5, 51.8, 59.1, and 57.5 µm (see Fig. 3(b)), indicating that TIG welding produces a significantly thicker layer with an average thickness of 55.3 µm. The difference in the thickness of the new layer is attributed to the uneven diffusion between materials during the MIG welding process, as the shorter welding duration inhibits the formation of a homogeneous metallurgical bond [14].

Fig. 4 illustrates the microstructure of the carbide interface and newly formed layer from the MIG and TIG welding methods. In Fig. 5, SEM microstructure images reveal various phases present in the newly formed layer, which are consistent between both welding processes. These phases include a light gray phase, a dark gray phase, and a black phase. Based on the EDS analysis results shown in Table II, the light gray phase is identified as an area enriched with W, while the dark gray phase is enriched with Fe.

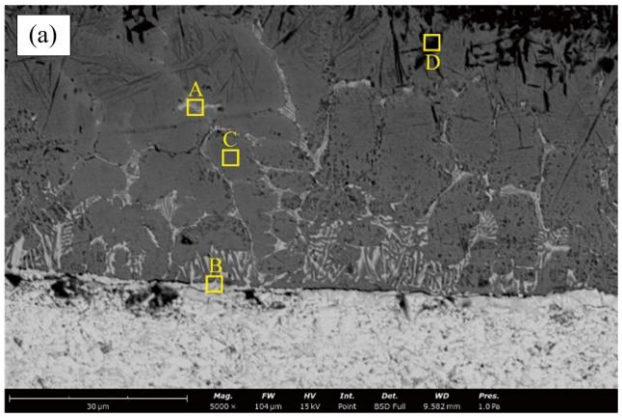

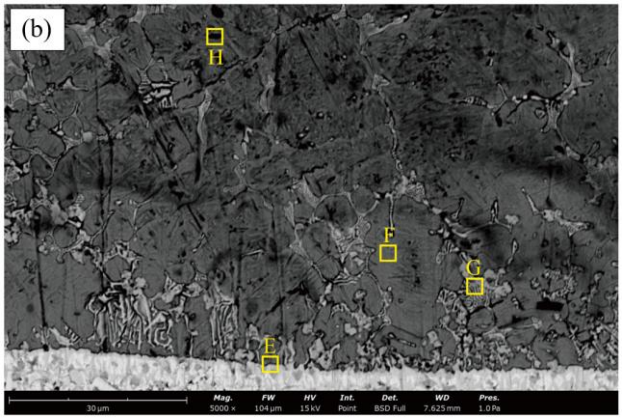

Fig. 4. The 5000× magnification of the welding results at the carbide interface showing the newly formed layer: (a) MIG and (b) TIG welding.

Additionally, the EDS analysis indicates that Fe is dominant throughout the new layer, with Table II confirming that Fe is evenly distributed due to the accelerated diffusion rate of Fe atoms at high temperatures [20]. The results of the EDS analysis for each phase are the same as the findings from other researchers [2, 21]. Filler metal alloys have a lower melting point compared to cemented carbide. During the welding process, the high temperatures melt the filler metal, which contains Fe elements that facilitate the formation of a diffusion layer. The diffusion of Fe elements results in the separation of W and C atomic particles from the cemented carbide, causing them to migrate along the interface as Fe atoms diffuse toward the center of the joint.

TABLE II. SEM-EDS POINT ANALYSIS OF MARKED LOCATIONS

Weight Conc	B	C	O	Mg	Si	Cr	Mn	Fe	Ni	Sr	W
A	-	15,763	2.008	0.100	-	0.201	-	48,695	0.100	0.803	32,329
B	-	35.8	5.4	0.1	-	-	-	27.0	0.4	-	31.3
C	-	22,078	2,597	0.200	-	-	-	61,738	0.200	-	13.187
D	-	35,365	4,595	0.100	1,399	-	-	54,745	0.799	-	2,593
E	3,103	17,117	1,401	0	-	0.200	-	11,411	0.601	-	66.166
F	4,605	14,414	1,401	-	-	0.601	-	65,666	0.300	-	13.013
G	3.424	22,457	7,452	0.000	-	0.201	-	25,579	0.403	-	40,483
H	2.603	28,228	7,708	0	-	0.601	1.101	54.154	0		4.905

Additionally, the high temperatures involved in the joining process lead to the decomposition of WC particles into W and C elements. Thus, the diffusion of C along the interface leads to the formation of distinct phases in the joint zone. The diffusion effect causes W and C atoms to migrate into the new layer region. However, the diffusion of W and C atomic elements due to the welding temperature does not extend into the filler metal layer, and the atomic elements within the filler metal do not diffuse into the carbide region [22]. The black phase observed in the microstructure is typically associated with the presence of carbon or carbon-rich compounds. In the context of welding processes involving cemented carbide, the black phase is often attributed to the formation of carbon-rich phases or carbides. During welding, the high temperatures can lead to the decomposition of the cemented carbide matrix, causing carbon to migrate and form new phases in the joint area. This migration can result in the appearance of a distinct black phase, which may represent the presence of carbon-rich precipitates or compounds formed as a result of the welding process.

In both MIG and TIG welding processes, the metallurgical bonds and distribution of atomic elements are confined to the newly formed layer. An additional observation from the EDS analysis of both welding methods is that cobalt (Co) from the carbide material does not diffuse into the new layer or the filler metal.

Fig. 5 presents SEM images of carbide and steel welded using lap joint configurations with MIG and TIG welding methods. Variations in welding speed, welding parameters, and the extent of the heat-affected zones significantly influence the SEM results, reflecting the

distinct effects of each welding method on the material interfaces. Fig. 5 presents SEM images of the Heat-Affected Zone (HAZ) for both MIG and TIG welding methods. These images demonstrate that both welding techniques effectively fill the gap between the carbide and steel materials, resulting in the formation of a new interfacial layer. The compound composition of this new layer differs depending on the welding method: Fe_2O_3 is formed during MIG welding, while $FeCO_3$ is produced during TIG welding. Quantitative measurements using ImageJ software indicate that the average thickness of the new layer is 63.38 µm for MIG welding and 62.09 µm for TIG welding. SEM analysis reveals that the newly formed interfacial layer between the carbide and steel is inhomogeneous, exhibiting defects in both welding methods. Specifically, cracks observed in MIG welding are located on the steel side of the interface, while in TIG welding, cracks propagate from the steel into the carbide. These cracks resulting from the welding process can significantly reduce the strength and integrity of the steel-carbide joint.

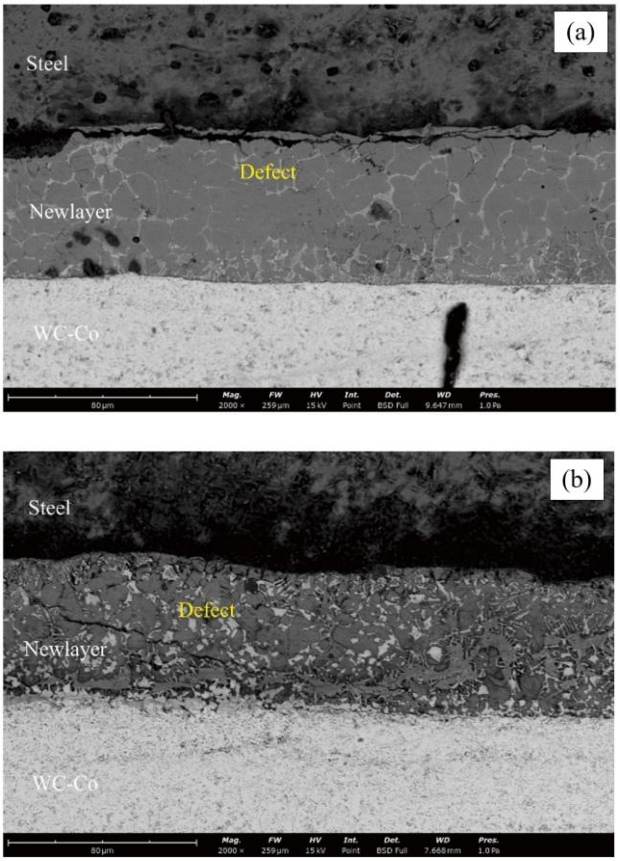

Fig. 5. Comparison of welding results between carbide and carbon steel interfaces (a) MIG and (b) TIG.

In MIG welding, Fe_2O_3 is an oxide that forms when iron reacts with oxygen at high temperatures. The presence of this oxide layer at the interface can lead to brittleness in the joint. Oxide layers are typically hard and brittle, which can initiate cracks under mechanical stress. It can act as a barrier to diffusion between the carbide and steel in the metallurgical bond.

To determine the formation of Fe_2O_3 (iron(III) oxide or hematite) during MIG welding, the EDS data were meticulously analyzed, focusing on the presence and atomic ratios of iron (Fe) and oxygen (O) within the samples. Fe_2O_3 is characterized by an ideal Fe molar ratio of 2:3, or approximately 0.67, which serves as a critical indicator for its identification. The detection of both Fe and O across the majority of samples indicates the potential formation of iron oxides. By calculating the Fe ratios in each sample where both elements are present, we can evaluate their alignment with the theoretical Fe ratio for Fe_2O_3. Consistent ratios near 0.67 across multiple samples would strongly support the presence of Fe_2O_3 rather than other iron oxides, such as FeO or Fe_3O_4, which have different stoichiometric ratios. This approach enables a robust assessment of Fe_2O_3 formation during MIG welding, providing valuable insights into the oxide layer's composition and structure.

In TIG welding, the $FeCO_3$ formation indicates a reaction between iron and carbon dioxide, leading to iron carbonate. This compound can decompose under welding temperatures to produce iron and carbon monoxide, facilitating better bonding. $FeCO_3$ does not form a brittle layer like Fe_2O_3. The absence of a brittle oxide layer allows for a more ductile joint that can absorb mechanical stresses without cracking. The formation of $FeCO_3$ contributes to a more uniform microstructure.

To verify the formation of $FeCO_3$ (iron(II) carbonate) during TIG welding, the elemental composition obtained from EDS data was analyzed, focusing on the presence and stoichiometric ratios of iron (Fe), carbon (C), and oxygen (O). $FeCO_3$ is characterized by a molar ratio of Fe:C:O of 1:1:3, which serves as a critical indicator for its formation. The atomic ratios were calculated by converting the weight percentages of Fe, C, and O into atomic ratios based on their respective atomic masses and normalizing them to assess alignment with the theoretical stoichiometric ratio. The consistent detection of Fe, C, and O across TIG-welded samples indicates the potential for carbonate formation, and calculated Fe:C:O ratios close to 1:1:3 strongly support the hypothesis of $FeCO_3$ formation. However, deviations from this ratio may suggest the coexistence of $FeCO_3$ with other phases, such as metallic Fe, iron oxides, or carbides. These findings provide compelling evidence for $FeCO_3$ formation under TIG welding conditions.

The compounds formed during welding significantly affect the durability of carbide and steel joints. Fe_2O_3 formation in MIG welding can lead to a weaker, more brittle joint prone to corrosion and mechanical failure. In contrast, $FeCO_3$ formation in TIG welding promotes a stronger, more durable joint with enhanced mechanical properties. Therefore, TIG welding may be the preferred method when joint durability is a critical consideration.

B. Hardness Distribution

Fig. 6 presents the hardness distribution results obtained using the micro Vickers hardness test across the materials—carbon steel, filler metal, and carbide—in both TIG and MIG welding. The hardness values differ among these materials depending on the welding method

used. It is observed that the parent metal regions of steel and carbide adjacent to the filler alloy and affected by the Heat-Affected Zone (HAZ) exhibit increased hardness compared to the regions not exposed to heat. This increase in hardness is attributed to the diffusion of alloying elements such as tungsten (W), carbon (C), iron (Fe), cobalt (Co), and nickel (Ni) within the solid-state phases. The phase formed around the interface between the cemented carbide and steel involves two simultaneous processes—nucleation and coalescence—during the joining process, resulting in the growth of new phases in the liquid state [11].

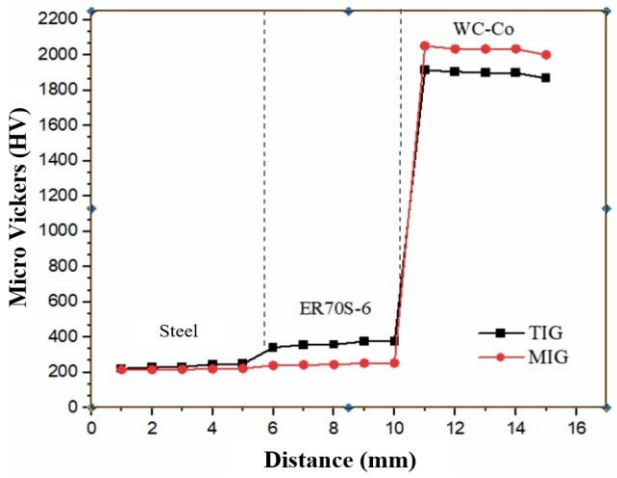

Fig. 6. Distribution of micro hardness values on steel specimens with comet carbide/WC-Co obtained by TIG and MIG welding methods.

Fig. 6 shows that the highest hardness value of 2051.8 HV is observed in the cemented carbide section when using the MIG welding method. This hardness decreases toward the filler metal section. The averaged test results reveal that the hardness value in the filler metal section is 361.6 HV for the TIG welding method, compared to 246.8 HV for the MIG welding method. The higher hardness achieved with the TIG welding method can be attributed to a more uniform heat distribution due to the lower welding speed. This slower speed allows the filler metal to fill the gap (≥0.5 mm) adequately, enhancing the metallurgical bond and preventing porosity in the melted filler metal [23]. The difference in hardness values between the two welding methods is 114.8 HV or approximately 31.74%. The hardness values obtained from the filler metal ER70S-6 in the filler metal area using both TIG and MIG welding methods are comparable to those reported in previous studies. Specifically, the investigation by Amirnasiri *et al.* [24] reported hardness values at the joint center ranging from 270 to 280 VHN when using RB CuZn-D foil filler metal with the brazing connection method. Additionally, Guimarães *et al.* [25] utilizing the Laser Powder Bed Fusion welding method with 316L stainless steel filler metal achieved hardness values between 238 HV and 302 HV.

Hardness measurements of the WC-Co cemented carbide section in both joining methods showed an increase at the 11 mm point, followed by a continuous decrease up to the 15 mm point. This decrease in hardness is attributed to the formation of solid solutions of intermetallic compounds resulting from reaction and diffusion processes [26]. Additionally, the central part of the layer includes a ductile interlayer, which can alleviate residual stresses and absorb external impacts through plastic deformation. The presence of hard phases within the joint enhances its stiffness due to their high hardness. Based on the results of hardness testing for both TIG and MIG welding methods, it is evident that the highest average hardness value in the filler metal area is achieved with TIG welding.

C. Shear Strength

Fig. 7 presents the shear strength test results for TIG and MIG welding, revealing that fractures occur in the cemented carbide area. The welding process induces differences in thermal expansion between the cemented carbide and steel, leading to residual stresses at the carbide joint and increased brittleness at the cemented carbide/filler metal interface. These factors result in fracture conditions observed during the shear strength test in the carbide section [27].

Additionally, the high temperatures generated during welding can weaken the joint strength by causing coarsening and grain growth of the WC grains. An increase in the grain size of WC-Co can significantly reduce the strength of the WC-Co material [28]. The main factors contributing to joint fracture include the phase distribution in the filler metal layer and defects in WC-Co caused by carbon diffusion [29].

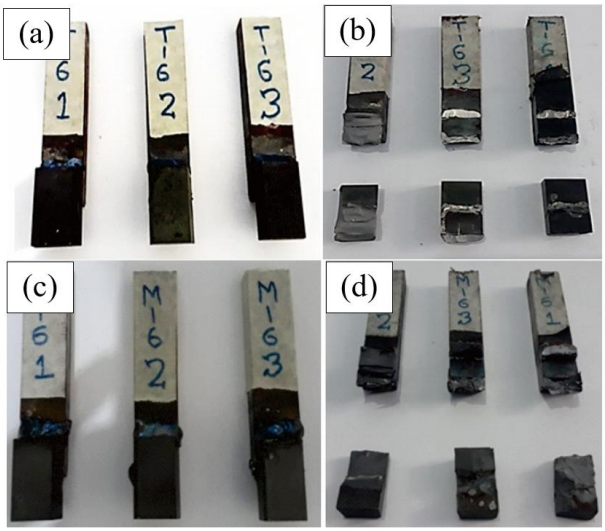

Fig. 7. The test results for (a) TIG welding before and (b) after shear strength testing, and (c) MIG welding before and (d) after shear strength testing.

In the averaged shear strength test data for each specimen, carbon steel and cemented carbide materials joined using TIG and MIG welding exhibit varying shear strength values. Fig. 8 shows that the highest shear strength value was obtained from MIG welding. Both TIG and MIG welding processes significantly influence the shear strength outcomes. The average shear strength for TIG welding was 379.5 MPa, with the fracture

occurring in the weld metal near the carbide, indicating a strong bond between the carbide and the filler metal. MIG welding exhibited a slightly higher average shear strength of 387.4 MPa, representing a 2.03% difference compared to TIG welding.

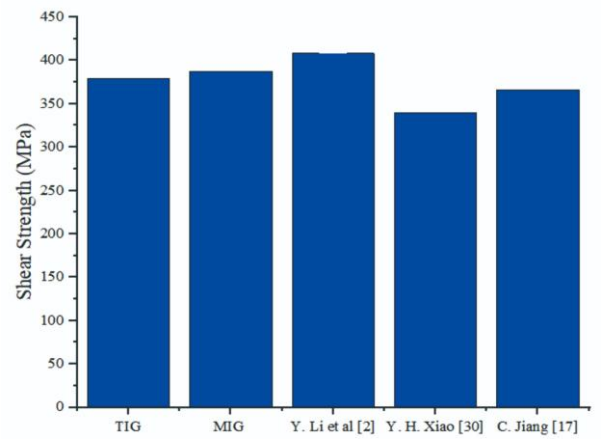

Fig. 8. Shear stress test graph on Tungsten Inert Gas (TIG) and Metal Inert Gas (MIG) welding.

The shear strength results align with those reported in previous research [2], where a shear strength of 408 MPa was achieved using the hybrid ultrasonic frequency induction welding method for cemented carbide/35CrMo material with Ag-Cu-Zn-Mn filler metal. Additionally, strength values of approximately 340 MPa were obtained for brazed joints with La_2O_3 additives [30, 31], and a maximum shear strength of 366 MPa was recorded for brazed joints at 770 °C for 30 s [17, 32].

These comparative studies indicate that high temperatures during the brazing process can produce maximum shear strength in joining cemented carbide and steel. Similarly, the TIG and MIG welding processes, which also operate at elevated temperatures, achieve strong metallurgical bonds when using ER70S-6 filler metal.

V. Conclusion

This study examined the effects of TIG and MIG welding on the joining of carbon steel and cemented carbide materials. The following conclusions can be drawn from the research:

1. Microstructural Observations: Both MIG and TIG welding processes successfully filled the narrow gap between cemented carbide and carbon steel; however, the resulting metallurgical bonds were not entirely homogeneous, and visible cracks were observed, particularly in MIG welding. The interface between the cemented carbide and the filler metal formed a new layer with an average thickness of 42.1 µm for MIG welding and 104.5 µm for TIG welding. Despite the formation of a new layer, the bond was inhomogeneous, with cracks predominantly observed in the MIG process.
2. Elemental Distribution: EDS analysis revealed that the new layers formed in both welding processes were enriched with C, O, Fe, and W elements. The elemental composition was similar across both methods, indicating consistent diffusion of atomic elements during welding.
3. Hardness Testing: Significant differences were observed in the hardness values between the weld metal and cemented carbide sections for TIG and MIG welding. In the weld metal, TIG welding produced a hardness of 361.6 HV, whereas MIG welding resulted in a hardness of 246.8 HV, with a difference of 31.74%. For the cemented carbide section, TIG welding yielded a hardness of 1897.4 HV, while MIG welding showed a higher hardness of 2031.6 HV, with a difference of 6.6%.
4. Shear Strength Testing: The results of the shear strength tests demonstrated minor differences between the two welding methods. TIG welding achieved a shear strength of 379.5 MPa, while MIG welding exhibited a slightly higher shear strength of 387.4 MPa, reflecting a difference of 2.03%. Visual inspection of the fracture patterns indicated that fractures predominantly occurred in the cemented carbide material for both TIG and MIG welding specimens.

Both TIG and MIG welding processes can effectively join carbon steel and cemented carbide. TIG welding results in a more uniform metallurgical bond and higher hardness in the weld metal. However, MIG welding produces a slightly higher shear strength, albeit with more visible cracks in the joint. These findings highlight the trade-offs between the two methods in terms of bond quality, hardness, and mechanical strength.

Conflict of Interest

The authors declare no conflict of interest.

Author Contributions

FEH was instrumental in conducting the essential specimen preparation and SEM-EDS analysis, facilitating the thorough investigation of microstructures. ADA, with careful precision, tackled the challenging process of manuscript composition, ensuring that our findings were clearly and thoroughly described. All authors had approved the final version.

Funding

The project received funding from the Ministry of Education, Culture, Research, and Technology of the Republic of Indonesia through the Thesis Magister Research Program under contract No: 007/LL6/PB/AL.04/2024, 196.83/A.3-III/LRI/VI/2024.

Acknowledgment

The authors express their gratitude to Universitas Muhammadiyah Surakarta and the Directorate of Research, Technology, and Community Service of the Republic of Indonesia for their substantial financial support of the research. Moreover, they would like to convey their appreciation to the Mechanical Engineering

Department and Material Laboratory for their significant contributions to the project.

REFERENCES

[1]. I. L. Velo, F. J. Gotor, M. D. Alcalá, C. Real, and J. M. Córdoba, "Fabrication and characterization of WC-HEA cemented carbide based on the CoCrFeNiMn high entropy alloy," *J. Alloys Compd.*, vol. 746, pp. 1–8, May 2018. doi: 10.1016/j.jallcom.2018.02.292

[2]. Y. Li *et al.*, "WC particulate reinforced joint by ultrasonic-associated brazing of WC-Co/35CrMo," *J. Mater. Process. Technol.*, vol. 238, pp. 15–21, Dec. 2016. doi: 10.1016/j.jmatprotec.2016.06.037

[3]. H. Wang, D. Yang, X. Zhao, C. Chen, and Q. Wang, "Microstructure and bend strength of WC–Co and steel joints," *Sci. Technol. Weld. Join.*, vol. 10, no. 2, pp. 167–168, Apr. 2005 doi: 10.1179/174329305X36052

[4]. L. Chen, C. Zhang, Z. Guo, and G. Liu, "Monitoring the evolution of resistance-welded WC-10Co/B318 steel joint based on welding time," *Int. J. Refract. Met. Hard Mater.*, vol. 113, 106221, Jun. 2023. doi: 10.1016/j.ijrmhm.2023.106221

[5]. G. Chen, X. Shu, J. Liu, B. Zhang, B. Zhang, and J. Feng, "Electron beam hybrid welding-brazing of WC-Co/40Cr dissimilar materials," *Ceram. Int.*, vol. 45, no. 6, pp. 7821–7829, Apr. 2019. doi: 10.1016/j.ceramint.2019.01.088

[6]. N. K. Sharma, R. Kannan, J. Hogan, G. Fisher, and L. Li, "Progress in improving joint strength of brazed cemented carbides and steels," *Sci. Technol. Weld. Join.*, vol. 26, no. 5, pp. 420–437, Jul. 2021. doi: 10.1080/13621718.2021.1931764

[7]. M.-N. Avettand-Fènoël, T. Nagaoka, H. Fujii, and R. Taillard, "Characterization of WC/12Co cermet–steel dissimilar friction stir welds," *J. Manuf. Process.*, vol. 31, pp. 139–155, Jan. 2018. doi: 10.1016/j.jmapro.2017.11.012

[8]. Y. Guo, Y. Wang, B. Gao, Z. Shi, and Z. Yuan, "Rapid diffusion bonding of WC-Co cemented carbide to 40Cr steel with Ni interlayer: Effect of surface roughness and interlayer thickness," *Ceram. Int.*, vol. 42, no. 15, pp. 16729–16737, Nov. 2016. doi: 10.1016/j.ceramint.2016.07.145

[9]. X. Wang, D. Zhou, and P. Xu, "The WC-Co/Fe–Ni interface: Effect of holding time on the microstructure, grain size and grain growth mechanism," *Ceram. Int.*, vol. 45, no. 17, pp. 23320–23327, Dec. 2019. doi: 10.1016/j.ceramint.2019.08.031

[10]. M. Amelzadeh and S. E. Mirsalehi, "Dissimilar joining of WC-Co to steel by low-temperature brazing," *Mater. Sci. Eng. B*, vol. 259, 114597, Sep. 2020. doi: 10.1016/j.mseb.2020.114597

[11]. X. J. Zhao, P. T. Liu, C. H. Chen, D. X. Yang, and T. Kohsuke, "η phase formation mechanism at cemented carbide YG30/steel 1045 joints during tungsten-inert-gas arc welding," *Mater. Sci. Forum*, vol. 675–677, pp. 901–904, Feb. 2011. doi: 10.4028/www.scientific.net/MSF.675-677.901

[12]. C. Jiang, H. Chen, X. Zhao, S. Qiu, D. Han, and G. Gou, "Microstructure and mechanical properties of brazing bonded WC-15Co/35CrMo joint using AgNi/CuZn/AgNi composite interlayers," *Int. J. Refract. Met. Hard Mater.*, vol. 70, pp. 1–8, Jan. 2018. doi: 10.1016/j.ijrmhm.2017.08.021

[13]. X. Yu, D. Zhou, D. Yao, F. Lu, and P. Xu, "Fiber laser welding of WC-Co to carbon steel using Fe-Ni Invar as interlayer," *Int. J. Refract. Met. Hard Mater.*, vol. 56, pp. 76–86, Apr. 2016. doi: 10.1016/j.ijrmhm.2015.12.006

[14]. G. Ying, H. Gong, and P. Xu, "Migration behavior of tungsten carbide in the dissimilar joints of WC-TiC-Ni/304 stainless steel using robotic MIG welding," in *Transactions on Intelligent Welding Manufacturing*, S. Chen, Y. Zhang, Z. Feng, Eds, Springer, Singapore, 2018, pp. 145–163. doi: 10.1007/978-981-10-8330-3_9

[15]. H. Chen, K. Feng, S. Wei, J. Xiong, Z. Guo, and H. Wang, "Microstructure and properties of WC–Co/3Cr13 joints brazed using Ni electroplated interlayer," *Int. J. Refract. Met. Hard Mater.*, vol. 33, pp. 70–74, Jul. 2012. doi: 10.1016/j.ijrmhm.2012.02.018.

[16]. Y. Guo, B. Gao, G. Liu, T. Zhou, and G. Qiao, "Effect of temperature on the microstructure and bonding strength of partial transient liquid phase bonded WC–Co/40Cr joints using Ti/Ni/Ti interlayers," *Int. J. Refract. Met. Hard Mater.*, vol. 51, pp. 250–257, Jul. 2015. doi: 10.1016/j.ijrmhm.2015.04.018

[17]. C. Jiang, H. Chen, Q. Wang, and Y. Li, "Effect of brazing temperature and holding time on joint properties of induction brazed WC-Co/carbon steel using Ag-based alloy," *J. Mater. Process. Technol.*, vol. 229, pp. 562–569, Mar. 2016. doi: 10.1016/j.jmatprotec.2015.09.044

[18]. Y. Winardi, Triyono, and A. T. Wijayanta, "Effect of filler and heat treatment on the physical and mechanical properties of the brazed joint between carbide tip and steel," *IOP Conf. Ser. Mater. Sci. Eng.*, vol. 176, 012026, Feb. 2017. doi: 10.1088/1757-899X/176/1/012026

[19]. K. Weman, "TIG welding," in *Welding Processes Handbook*, Elsevier, 2012, pp. 63–69. doi: 10.1533/9780857095183.63

[20]. J. Zhang, Q. Shen, G. Luo, M. Li, and L. Zhang, "Microstructure and bonding strength of diffusion welding of Mo/Cu joints with Ni interlayer," *Mater. Des.*, vol. 39, pp. 81–86, Aug. 2012. doi: 10.1016/j.matdes.2012.02.032

[21]. M. Amelzadeh and S. E. Mirsalehi, "Influence of braze type on microstructure and mechanical behavior of WC-Co/steel dissimilar joints," *J. Manuf. Process.*, vol. 36, pp. 450–458, Dec. 2018. doi: 10.1016/j.jmapro.2018.10.015

[22]. S. D. Agung *et al.*, "Effect of Shielded metal arc welding on microstructure, hardness, and tensile strength of nodular cast iron," *Advances in Science and Technology*, vol. 141. pp. 21–26, 2024. doi: 10.4028/p-2gxSXr

[23]. B. Ma, X. Wang, C. Chen, D. Zhou, P. Xu, and X. Zhao, "Dissimilar welding and joining of cemented carbides," *Metals (Basel).*, vol. 9, no. 11, 1161, Oct. 2019. doi: 10.3390/met9111161

[24]. A. Amirnasiri, N. Parvin, and M. S. haghshenas, "Dissimilar diffusion brazing of WC-Co to AISI 4145 steel using RBCuZn-D interlayer," *J. Manuf. Process.*, vol. 28, pp. 82–93, Aug. 2017. doi: 10.1016/j.jmapro.2017.06.001

[25]. B. Guimarães *et al.*, "WC-Co/316L stainless steel joining by laser powder bed fusion for multi-material cutting tools manufacturing," *Int. J. Refract. Met. Hard Mater.*, vol. 112, 106140, Apr. 2023. doi: 10.1016/j.ijrmhm.2023.106140

[26]. T. W. B. Riyadi *et al.*, "Fabrication of NiAl and TiC intermetallic matrix composite coatings," *Compos. Interfaces*, vol. 29, no. 3, pp. 328–343, 2022. doi: 10.1080/09276440.2021.1942667

[27]. L. Pintschovius, B. Schreieck, B. Eigenmann, and D. Löhe, "Residual stresses in brazed joints of cemented carbide and steel with complex geometry," *Mater. Sci. Forum*, vol. 347–349, pp. 652–657, May 2000. doi: 10.4028/www.scientific.net/MSF.347-349.652

[28]. M. Zhu *et al.*, "A novel method for direct synthesis of WC-Co nanocomposite powder," *Metall. Mater. Trans. A*, vol. 42, no. 9, pp. 2930–2936, Sep. 2011, doi: 10.1007/s11661-011-0681-4

[29]. Z. Zheng *et al.*, "Interfacial microstructure and mechanical properties of WC–Co/40Cr joints brazed at low–temperature with Ag–Cu–Ti + Sn novel filler," *Vacuum*, vol. 212, 111988, Jun. 2023. doi: 10.1016/j.vacuum.2023.111988

[30]. Y. H. Xiao, P. W. Liu, Z. Wang, Y. Wang, K. Q. Feng, and L. Chen, "La_2O_3 addition for improving the brazed joints of WC-Co/1Cr13," *J. Mater. Process. Technol.*, vol. 267, pp. 17–25, May 2019. doi: 10.1016/j.jmatprotec.2018.11.045

[31]. A. Yulianto, A. S. Darmawan, A. D. Anggono, and R. F. Scannov, "The effect of nodular graphite on hardness and toughness in permanent molds made of ferro casting ductile," *Journal of Physics: Conference Series*, vol. 2739, no. 1. 2024. doi: 10.1088/1742-6596/2739/1/012035

[32]. W. S. Liu, Q. S. Cai, Y. Z. Ma, Y. Y. Wang, H. Y. Liu, and D. X. Li, "Microstructure and mechanical properties of diffusion bonded W/steel joint using V/Ni composite interlayer," *Mater. Charact.*, vol. 86, pp. 212–220, Dec. 2013. doi: 10.1016/j.matchar.2013.10.013